Influence of an Exocyclic Guanine Adduct on the Thermal Stability, Conformation, and Melting Thermodynamics of a DNA Duplex†

G. Eric Plum,‡ Arthur P. Grollman,§ Frances Johnson,§ and Kenneth J. Breslauer*,‡

Department of Chemistry, Rutgers, The State University of New Jersey, New Brunswick, New Jersey 08903, and Department of Pharmacological Sciences, State University of New York at Stony Brook, Stony Brook, New York 11794

Received June 4, 1992; Revised Manuscript Received September 28, 1992

ABSTRACT: As part of an overall program to characterize the impact of mutagenic lesions on the physiochemical properties of DNA, we report here the results of a comparative spectroscopic study on pairs of DNA duplexes both with and without an exocyclic guanine lesion. Specifically, we have studied a family of four 13-mer duplexes of the form d(CGCATGYGTACGC)·d(GCGTACZCATGCG) in which Y is either the normal deoxyguanosine residue (G) or the exocyclic guanine adduct 1,N^2-propanodeoxyguanosine (X), while Z is either deoxycytosine (C) or deoxyadenosine (A). Thus, the four duplexes studied, which can be designated by the identity of their central Y·Z base pair, are a Watson–Crick duplex (GC), a duplex with a central mismatch (GA), and two duplexes with exocyclic guanine lesions (X), that differ only by the base opposite the lesion (XC and XA). The data derived from our spectroscopic measurements on these four duplexes have allowed us to evaluate the influence of the exocyclic guanine lesion, as well as the base opposite the lesion, on the conformation, thermal stability, and melting energetics of the host DNA duplex. To be specific, our circular dichroism (CD) spectra show that the exocyclic guanine lesion induces alterations in the duplex structure, while our temperature-dependent optical measurements reveal that these lesion-induced structural alterations reduce the thermal stability, the transition enthalpy, and the transition free energy of the duplex. We also find that the lesion-induced thermal destabilization of the duplex (ΔT_m) primarily results from the presence of the modified guanine residue, while being relatively insensitive to whether the base opposite the lesion is a C or an A residue (e.g., XA and XC have the same T_m values). In other words, the presence of the lesion makes the duplex thermal stability insensitive to the base opposite it, a result that contrasts with the corresponding unmodified duplexes GA and GC which exhibit substantially different T_m values. By contrast, we find that the presence of the lesion does *not* alter the influence of the cross-strand partner on the duplex differential thermodynamic stability, $\Delta\Delta G$. In other words, the GC and GA duplexes and the XC and XA duplexes exhibit identical differences in free energy ($\Delta\Delta G$). Thus, the lesion alters the differential thermal stability (ΔT_m) but not the differential thermodynamic stability ($\Delta\Delta G$) of duplexes with C and A cross-strand partners. Our CD spectra reveal an intriguing pH-dependent structural transition with an apparent pK_a near neutrality for the XA duplex which is absent in the other three duplexes. Because A residues are inserted preferentially opposite X lesions in vivo, this result suggests that the biological repair system may be confronted with a mixture of two structures under physiological conditions. We also find the XA and XC duplexes to be thermodynamically similar. Consequently, the observed biological preference for insertion of A over C residues across from the lesion cannot be rationalized simply in terms of thermodynamic differences between the final duplex states. Finally, our data reveal the thermodynamic consequences of the pH-induced, structural alterations in the XA duplex observed by NMR (Kouchakdjian et al., 1989, 1990) to be minimal. This surprising result suggests that DNA may be sufficiently plastic so as to accommodate significant structural alterations in a compensatory manner so as to minimize the net energetic cost.

As part of our overall program to characterize the impact of mutagenic lesions on the physiochemical properties of DNA (Vesnaver et al., 1989), we are investigating the effect of an exocyclic guanine adduct on the thermodynamics and conformational preferences of an oligomeric DNA duplex. Exocyclic adducts are believed to be important in mutagenesis and carcinogenesis (Shapiro, 1969; Singer & Grunberger, 1983; Singer & Bartsch, 1986; Basu & Essignmann, 1988). Chung et al. (1984) have demonstrated that exocyclic adducts of guanine form when deoxyguanosine, either free or incorporated into DNA, is exposed to acrolein, a common environmental pollutant.

Despite the postulated significance of exocyclic adducts as agents of mutagenesis and carcinogenesis (Singer & Bartsch, 1986), only recently has detailed structural information on such lesions become available through NMR studies on modified oligomeric duplexes (Kouchakdjian et al., 1989, 1990, 1991). These NMR studies are designed to characterize the structural distortions induced within the host duplex by the exocyclic adduct. Such structural information is expected to provide insight into the recognition and repair of exocyclic adducts by the cellular machinery involved in DNA repair and replication. By contrast, no systematic thermodynamic study has been reported on DNA structures containing exocyclic adducts. Thus, despite the emergence of a structural picture, it is not yet possible to evaluate quantitatively the influence of an exocyclic lesion on the stability and the melting behavior of a DNA duplex. Such assessments require thermodynamic data on DNA duplexes both with and without

† This research was supported by NIH Grants CA-47795 (A.P.G. and K.J.B.), GM-23509, and GM-34469 (K.J.B.).

‡ Rutgers, The State University of New Jersey.

§ State University of New York at Stony Brook.

0006-2960/92/0431-12096$03.00/0 © 1992 American Chemical Society

Table I: Thermal and Thermodynamic Melting Properties of Duplexes with and without an Exocyclic Guanine Lesion[a]

duplex	T_m[b] (°C)	ΔT_m[c] (°C)	ΔH_{vH} (kcal/"mole")	$T\Delta S_{vH}$ (kcal/"mole")	ΔG_{vH} (kcal/"mole")	$\Delta\Delta G_{vH}$[d] (kcal/"mole")
5'-CGCATGGGTACGC-3' GC 3'-GCGTACCCATGCG-5'	63.6		101.0 ± 2.2 (10)	83.2 ± 2.1	17.8 ± 0.3	
5'-CGCATGGGTACGC-3' GA 3'-GCGTACACATGCG-5'	57.4	6.2	92.2 ± 1.6 (10)	75.7 ± 1.5	16.5 ± 0.2	1.3 ± 0.5
5'-CGCATGXGTACGC-3' XC 3'-GCGTACCCATGCG-5'	50.7	12.9	87.9 ± 1.8 (10)	73.9 ± 1.5	14.0 ± 0.2	
5'-CGCATGXGTACGC-3' XA 3'-GCGTACACATGCG-5'	51.6	12.0	86.9 ± 3.0 (9)	74.2 ± 1.8	12.7 ± 0.2	1.3 ± 0.4

[a] All data were measured at pH 7.0 in a 10 mM pyrophosphate buffer containing 1 M NaCl and 1 mM EDTA. The error limits listed are standard errors. For ΔH_{vH}, the number of concentrations for which data are averaged is shown in parentheses. $T\Delta S_{vH}$ and ΔG_{vH} are for $T = 298$ K. The "mole" unit refers to mole of cooperative unit. [b] T_ms listed refer to a common total strand concentration, 6×10^{-6} M. [c] $\Delta T_m = T_m(GC) - T_m$. [d] $\Delta\Delta G_{vH} = \Delta G_{vH}(GC) - \Delta G_{vH}(GA)$ or $\Delta\Delta G_{vH} = \Delta G_{vH}(XC) - \Delta G_{vH}(XA)$.

the lesion. In conjunction with the recently emerging structural picture, such thermodynamic data should provide insights into the mechanism(s) by which exocyclic adducts exert their biological impact.

To obtain the requisite thermodynamic data, we have conducted a comparative spectroscopic investigation on the family of DNA duplexes shown in Table I. These duplexes differ by the presence or absence of a centrally located X residue (where X represents the 1,N^2-propanodeoxyguanosine moiety, a stable analogue of the exocyclic guanine adducts formed by reaction with acrolein), and by the identity of the base opposite the lesion. All of the spectroscopic studies described herein were performed over a range of pH from 6.0 to 9.6, thereby vastly increasing the number of measurements required to obtain a complete picture of the impact of the exocyclic lesion. This feature of the study is necessary, however, because the NMR data of Patel and co-workers (Kouchakdjian et al., 1989, 1990) and the molecular dynamics calculations of Huang and Eisenberg (1992) reveal the exocyclic lesion to exhibit structural properties that are pH-dependent.

The abbreviations for and the sequences of the duplexes we have studied are listed in Table I. Note that these abbreviations simply designate the identity of the central base pair (shown in boldface), the entity which differentiates one duplex from another. An examination of the sequences reveals that we have studied two modified duplexes containing the X lesion opposite deoxyadenosine and deoxycytidine residues (XA and XC), and the corresponding two unmodified parent duplexes (GA and GC). For the reasons described below, these four duplexes were selected for the studies reported here.

At the time of lesion formation in vivo, the base opposite the modified guanine is cytosine. Thus, a comparison of the properties of the XC- and GC-containing duplexes will provide insight into the consequences of a nascent lesion. In vitro and in vivo studies of replication demonstrate that deoxyadenosine is placed preferentially opposite the 1,N^2-propanodeoxyguanosine lesion (Grollman, 1989). Thus, a comparison of the properties of the XA- and GA-containing duplexes may elucidate a thermodynamic/structural origin for this preference. Is the deoxyadenosine preference due to enhanced stability of the XA duplex relative to duplexes with other bases opposite the lesion, or is the preference a consequence of some property of the polymerase itself, or both?

In summary, we report here the results of a comparative, pH-dependent spectroscopic study of a Watson–Crick duplex (GC), a mismatch duplex (GA), and two duplexes with exocyclic guanine lesions, that differ only by the base opposite the lesion (XC and XA). The data derived from these studies enable us to evaluate quantitatively the pH-dependent influence of an exocyclic lesion and the base opposite it on the conformation, the thermal stability, and the melting thermodynamics of a DNA duplex. Because Patel and co-workers (Kouchakdjian et al., 1989, 1990) have used NMR to map the pH-dependent solution structures of a duplex essentially identical to one of the four duplexes studied here (XA), our results also provide a unique opportunity to correlate macroscopic thermal and thermodynamic data with microscopic structural information.

MATERIALS AND METHODS

Oligonucleotide Synthesis. The oligonucleotide containing the exocyclic adduct, 1,N^2-propanodeoxyguanosine, was prepared and purified as described by Kouchakdjian et al. (1989). The remaining three oligonucleotides were synthesized and purified as described by Plum et al. (1990).

Buffer Conditions and pH Adjustment. To maintain satisfactory hydrogen ion buffer capacity over the wide ranges of pH and temperature explored in this study, pyrophosphate was employed as buffer. All experiments, with the exception of the CD measurements, were carried out in solutions containing 10 mM pyrophosphate, 1 M NaCl, and 1 mM EDTA. For collection of CD spectra, the buffer contained 0.1 mM EDTA. Adjustment of pH was accomplished by addition of microliter quantitites of 1.0 M HCl or NaOH, as appropriate.

Determination of Extinction Coefficients. The molar extinction coefficient for each oligonucleotide was determined by phosphate analysis (Snell & Snell, 1949). The stoichiometry of oligonucleotide complexation and the molar extinction coefficients for the complexes were determined by the method of continuous fractions (Job, 1928; Felsenfeld & Rich, 1957). Concentrations of single- and double-stranded oligonucleotides were calculated from the absorbance at 260 nm and the measured extinction coefficients.

UV Melts. Ultraviolet absorbance thermal melting profiles were collected as a function of pH and oligonucleotide concentration. The pH-dependent data were collected on a Perkin-Elmer 575 spectrophotometer equipped with thermoelectric temperature control and interfaced to a Techtronix 4051 computer. The temperature was increased at a rate of 0.5 °C/min. The temperature and absorbance at 260 nm were read and stored at 30-s intervals. Extraction of melting temperatures (T_m) and van't Hoff transition enthalpies (ΔH_{vH}), entropies (ΔS_{vH}), and free energies (ΔG_{vH}) from the experimental absorbance versus temperature melting curves was accomplished as previously described (Marky & Breslauer,

1987), using the standard assumptions of two-state, bimolecular behavior, and a zero net change in heat capacity for the transition. To be specific, values for ΔH_{vH} were determined from the shapes of the melting curves (Marky & Breslauer, 1987), while the corresponding entropies were estimated from $\Delta S_{vH} = \Delta H_{vH}/T_m - R \ln (4C_T)$, where R is the gas constant and C_T is the total oligonucleotide strand concentration. The free energy then was calculated using $\Delta G_{vH} = \Delta H_{vH} - T\Delta S_{vH}$.

We also measured the dependence of T_m on the total oligonucleotide strand concentration (C_T). These studies were performed using a Perkin-Elmer Lambda 4c spectrophotometer interfaced with a National Instruments GPIB-SCSI controller to an Apple Macintosh computer. The temperature was controlled by a Perkin-Elmer digital controller identical to that used with the Model 575. The temperature was monitored by a Keithley Model 177 digital multimeter equipped with a Model 1793/6423 IEEE standard output device interfaced to the GPIB-SCSI controller. For the melting of relatively short oligonucleotide duplexes, one generally can calculate ΔH_{vH} from the slope of $1/T_m$ versus log C_T plots (Cantor & Schimmel, 1980). However, due to the approach of the pseudomonomolecular melting behavior characteristic of polymeric duplexes, we found the T_m dependence on C_T to be reduced artificially for the duplexes studied here, thereby precluding use of this method for deriving ΔH_{vH} values. Such behavior previously has been noted for duplexes with chain lengths greater than about 12 (Breslauer et al., 1975; Marky et al., 1987). Consequently, in this work we have calculated ΔH_{vH} by analyzing the shapes of the UV melting curves. This method for calculating ΔH_{vH} for oligonucleotide transitions normally is less desirable than calculations based on the slope of $1/T_m$ versus log C_T plots. However, for oligomeric duplexes of the chain length studied here, determining ΔH_{vH} by analyzing the shape of individual melting curves has the advantage of not being compromised by approach to the pseudomonomolecular melting behavior characteristic of polymer duplexes.

Circular Dichroism. Circular dichroism (CD) spectra at pH 7.0 were collected from 200 to 350 nm at 0.5-nm intervals with a 10-s averaging time on an Aviv Model 60 DS spectropolarimeter (Aviv Associates, Lakewood, NJ) at neutral pH and 25 °C. The concentration of DNA duplex was $\sim 2 \times 10^{-5}$ M. A 0.1-cm path-length cell was used.

CD spectra, as a function of pH, were collected as described above, except the DNA duplex concentration was $\sim 3 \times 10^{-5}$ M. The pH was adjusted by addition of microliter quantities of 1.0 M HCl or NaOH, as appropriate. To analyze the pH-dependent CD data, we assumed a model consistent with the NMR data (Kouchakdjian, 1989, 1990) in which there is an equilibrium between a single high-pH and a single low-pH structure, each of which exhibits a unique CD spectrum. With this two-state assumption, the course of the CD-detected titration curve, at any wavelength, may be described by the equation:

$$[\theta] = \frac{[\theta]_{\text{low pH}} + [\theta]_{\text{high pH}} 10^{\text{pH}-\text{p}K}}{1 + 10^{\text{pH}-\text{p}K}} \quad (1)$$

where $[\theta]_{\text{high pH}}$ and $[\theta]_{\text{low pH}}$ are the limiting molar ellipticities at high and low pH, respectively. The pH-dependent molar ellipticity data we measured were fit to this equation by standard nonlinear least-squares techniques.

RESULTS AND DISCUSSION

The Exocyclic Lesion Weakly Perturbs the CD Profile of the Host Duplex at Neutral pH. Inspection of the CD spectra shown in Figure 1 reveals that the lesion-containing duplex, XC, exhibits a somewhat altered CD profile relative to its Watson–Crick parent duplex, GC, particularly at wavelengths below 260 nm. This observation suggests that the exocyclic lesion perturbs the conformation of the host duplex, a conclusion which is consistent with the NMR evidence of Patel and co-workers on a similar lesion-containing duplex (Kouchakdjian et al., 1989, 1990). Significantly, in this work, we also have studied the parent GC duplex, thereby providing the opportunity for a direct comparison between the properties of the duplex both with (XC) and without (GC) the modified guanine residue.

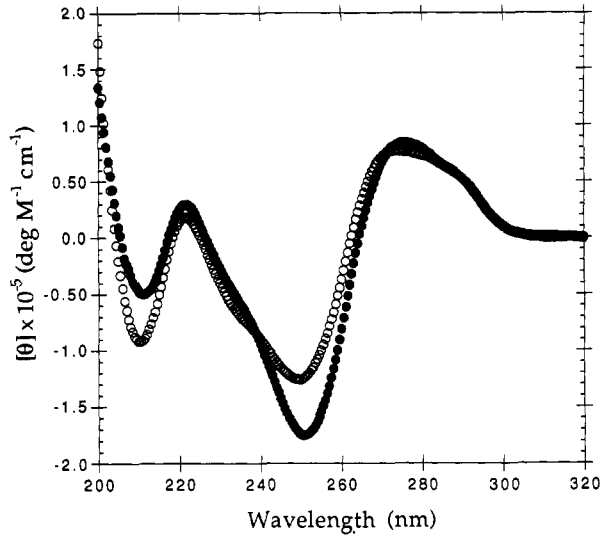

FIGURE 1: Circular dichroism of GC (○) and XC duplexes (●) at neutral pH. The molar ellipticity in this and all subsequent CD curves refers to the total strand concentration, C_T.

The aforementioned lesion-induced perturbation of duplex structure should be considered when developing molecular interpretations of how repair enzymes recognize a lesion-containing DNA domain. It should be noted, however, that the CD-detected, lesion-induced, structural perturbation is relatively subtle, since both the GC and XC duplexes exhibit CD spectral shapes characteristic of global B-like DNA structures (Bush, 1974). This conclusion also is consistent with the NMR data of Patel and co-workers on a similar lesion-containing duplex. They also find that the global duplex conformation remains B-like despite the local structural perturbation induced by the exocyclic lesion (Kouchakdjian et al., 1989, 1990). In short, although more qualitative, our CD-derived conclusions concerning the impact of the exocyclic lesion on duplex structure are consistent with the corresponding NMR data. Interestingly, the CD spectra of the GA and XA duplexes, which are displayed in Figure 2, also suggest that modification of the guanine residue perturbs the structure of the duplex in which the cross-strand partner is an A rather than a C residue. Again the global duplex structures remain B-like. Thus, the CD-detected impact of guanine modification (the G to X transformation) on duplex structure qualitatively appears not to depend strongly on whether the base opposite the lesion is a C or an A residue.

The Exocyclic Lesion Thermally Destabilizes the Duplex at Neutral pH. Inspection of the T_m data listed in Table I reveals that the lesion-containing XC duplex exhibits a melting temperature that is ~13 °C lower than that of the corresponding unmodified Watson–Crick parent duplex, GC. Thus, the exocyclic lesion not only perturbs the isothermal duplex structure (as we observe by CD) but also induces a substantial reduction in the thermal stability of the host duplex.

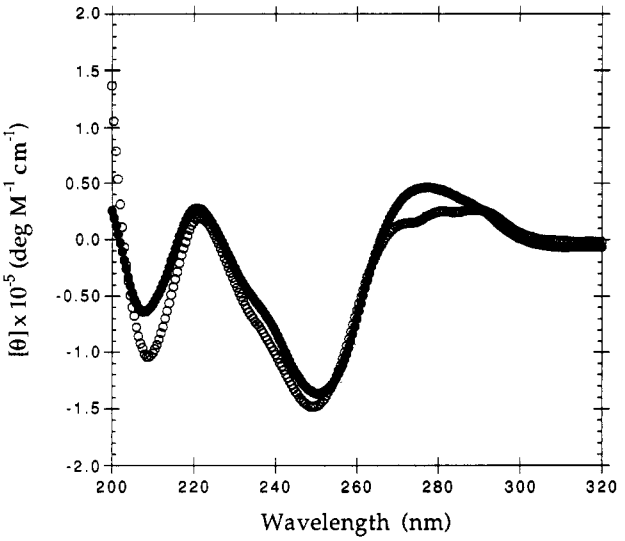

FIGURE 2: Circular dichroism of GA (○) and XA duplexes (●) at neutral pH.

The Lesion Makes the Thermal Stability of the Duplex Insensitive to Whether the Base Opposite the Modified Guanine Residue Is C or A. For unmodified DNA duplexes, conversion of a Watson–Crick base pair into a mismatch base pair results in a significant reduction in the duplex melting temperature (Aboula-ela et al., 1985; Gaffney & Jones, 1989). We, in fact, observe such behavior for the unmodified GC and GA duplexes, with the mismatch-containing GA duplex exhibiting a T_m which is ~6 °C below that of its parent Watson–Crick GC duplex (see Table I). By contrast, inspection of the T_m data in Table I reveals very similar melting temperatures for the two lesion-containing duplexes, XC and XA. Thus, the magnitude of the thermal destabilization (ΔT_m in Table I) is relatively insensitive to whether a C or an A residue is incorporated opposite the lesion. This observation suggests that the lesion-induced thermal destabilization primarily results from the presence of the exocyclic lesion and is relatively insensitive to whether the base opposite the propano-dG is C or A. Thus, the exocyclic lesion exerts an influence on the duplex DNA which is reflected in both the CD-detected isothermal structure and the temperature-dependent melting properties of the duplex.

The Lesion-Containing XA Duplex Exhibits a Unique pH-Dependent Structural Transition. The CD spectra of the GC, GA, and XC duplexes show no dependence on pH between 6.0 and 9.6. This observation, which is consistent with expectations, suggests that the global structures of these duplexes are insensitive to changes in pH over this range. By contrast, we find the CD spectrum for the XA duplex to be surprisingly sensitive to pH changes in this range.

By application of eq 1 to plots of ellipticity versus pH, we calculate an apparent pK_a of ~6.6 for the pH-induced structural transition in the XA duplex. Representative plots at four wavelengths are shown in Figure 3. Within experimental error, the apparent pK_a we observe is independent of wavelength (Figure 4), a result which supports our assumption that only two structures are present, and that they are in a pH-dependent equilibrium. These observations are consistent with the structural picture derived from NMR data which reveals a high- and a low-pH form for the lesion-containing XA duplex (Kouchakdjian et al., 1989, 1990). In addition, in this work we are able to demonstrate that this pH-dependent behavior is unique to the XA duplex since we also have studied the corresponding GC, GA, and XC duplexes in which no such pH-dependent transformation is observed over the pH range studied.

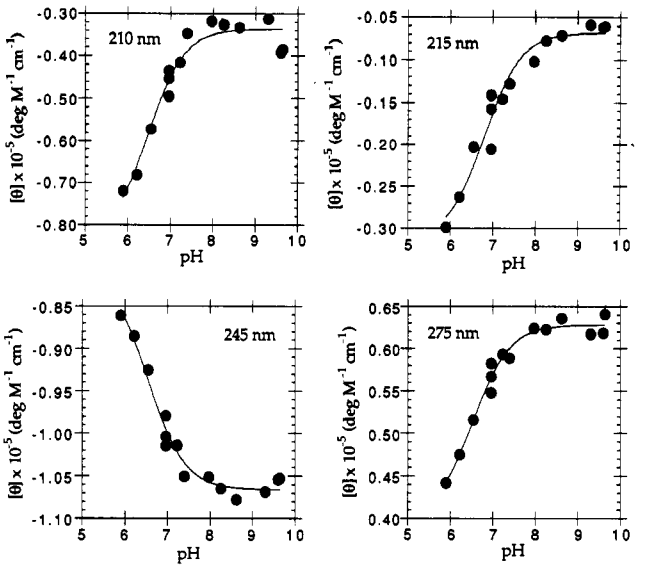

FIGURE 3: pH dependence of CD of the XA duplex at the indicated wavelength. (The solid lines were calculated using eq 1).

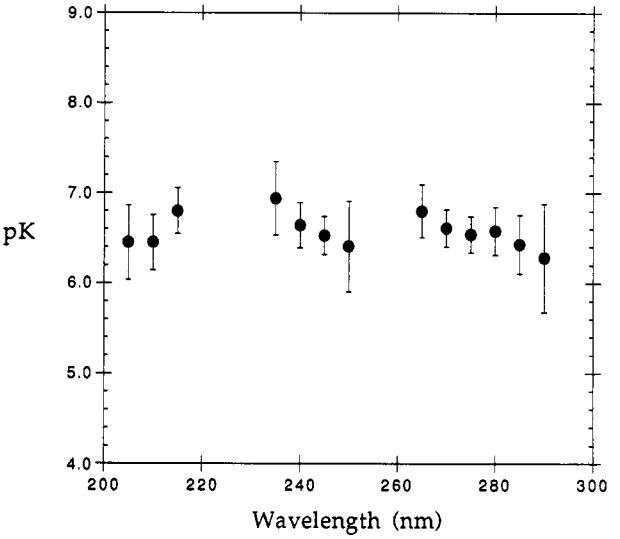

FIGURE 4: Wavelength dependence of the apparent pK_a of the CD-observed, pH-dependent structural transition of the XA duplex. Error bars indicate 95% confidence intervals for the fitted apparent pK_a.

The observation of a unique pH-induced structural transition for the XA duplex, with an apparent pK_a near neutrality, means that for this duplex the biological repair system may be confronted with a mixture of the two structures under physiological conditions. This intriguing feature must be considered when developing models for mechanisms by which the repair enzymes recognize and selectively bind to lesion-containing DNA domains.

The Influence of pH on Duplex Thermal Stability (T_m). Typically, DNA duplex thermal stability (T_m) is reduced at low and at high pH due to facilitated protonation/ionization of functional groups on the DNA bases which favor formation of single strands since the Watson–Crick hydrogen-bonding scheme may be disrupted and the net charge on the molecule changes. Consistent with this expectation, we find the T_m of each duplex to be dependent on pH over the range studied 6.0–9.6 (see Figure 5). Specifically, the T_m's for the four duplexes display a slight pH dependence between pH 6 and 8 and decline precipitously above pH 8. Significantly, however, the shapes of the curves do not depend on the central base pair. Consequently, the T_m trends we observe are not trivial functions of the pH value chosen for comparison.

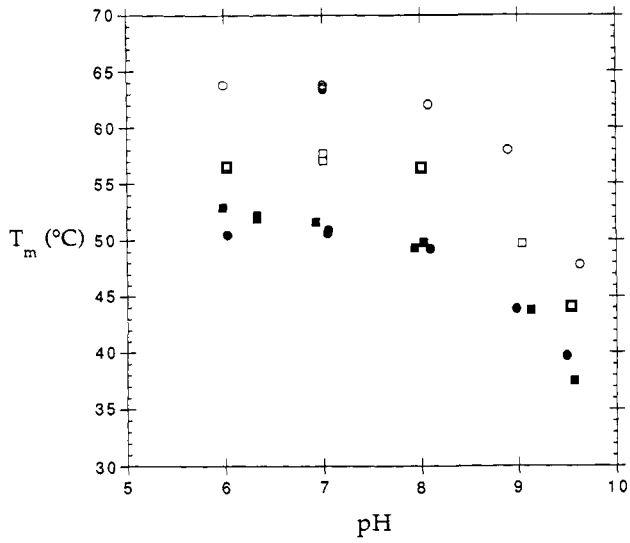

FIGURE 5: Dependence of the duplex thermal stability (T_m) on pH: GC (○), GA (□), XC (●), XA (■). Duplex concentration is 3 μM.

For the three duplexes for which no pH-dependent structural changes are observed between 6 and 9.6, the virtual identity of the T_m dependence on pH comes as no surprise. On the other hand, in this pH range, the XA base pair exhibits a major structural rearrangement, observable by NMR and CD (a proton is released and a potential hydrogen bond lost), yet we observe as a function of pH no significant change in the XA duplex thermal stability (T_m), relative to the XC duplex. This surprising observation, which may reflect compensating effects, will be discussed below when we compare our thermal and thermodynamic data with the structural picture. However, independent of our molecular interpretation, the absence of a significant difference in T_m for the XA and XC duplexes near neutral pH (despite the observation that the XA duplex, in contrast to its XC counterpart, is participating in a major structural transition) underscores the need to go beyond simple UV absorbance-based T_m measurements to elucidate the physiochemical impact of a lesion. In other words, the intriguing pH-dependent structural transition that we observe by CD and Patel observes by NMR in the XA duplex may not have been detected by simple UV absorbance-based T_m measurements.

The Exocyclic Lesion Reduces the Duplex Transition Enthalpy. From nearest-neighbor calculations (Breslauer et al., 1986), we predict a transition enthalpy of 107 kcal/mol for the thermally induced disruption of the GC duplex. By analyzing the shape of the UV absorbance melting profile of the GC duplex, we calculate a van't Hoff transition enthalpy, ΔH_{vH}, of 101.0 kcal/"mole". In light of the errors inherent in this analysis, this agreement between the predicted and "observed" values is quite good and lends credence to our use of this approach for obtaining ΔH_{vH} from UV melting curves. As expected, we find the ΔH_{vH} data obtained in this manner to be independent of concentration. By contrast, our $1/T_m$ versus log C_T plots exhibit slopes which are reduced relative to those expected from the ΔH_{vH} data we derived by analyzing the shapes of the UV melting curves. As noted earlier, a reduced concentration dependence of T_m is indicative of approach to the pseudomonomolecular melting behavior characteristic of polymers. For this reason, we derived our ΔH_{vH} data by analyzing the shapes of individual melting curves rather than from the concentration dependence of T_m.

Inspection of the van't Hoff enthalpy data listed in Table I reveals the thermally induced disruption of the XC duplex to be accompanied by a lower transition enthalpy than that associated with disruption of the unmodified GC duplex. In other words, the presence of the exocyclic lesion causes a reduction in the duplex transition enthalpy relative to the corresponding Watson–Crick duplex. We find a similar effect for the GA versus XA duplex. However, the magnitude of this lesion-induced reduction in ΔH_{vH} is less because the mismatch duplex (GA) already exhibits a reduced transition enthalpy relative to the fully-paired Watson–Crick parent GC duplex, an observation consistent with previous work (Gaffney & Jones, 1989; Aboul-ela et al., 1985). The significant point is that in both cases (GC vs XC and GA vs XA), incorporation of the exocyclic lesion via guanine modification (a G to X transformation) results in a reduced transition enthalpy for the lesion-containing duplex.

With the reasonable assumption that the high-temperature final states are energetically equivalent, these enthalpy data suggest that the CD- and NMR-detected, lesion-induced structural alterations of the duplex result in enthalpically unfavorable perturbations to the duplex state. Interpretations of these enthalpy data in terms of potential molecular/structural considerations will be presented in a later section.

Comparisons between the van't Hoff transition enthalpies described above implicitly assume that the "mole" melting entity is identical for the four duplexes studied, in other words, that the duplexes melt with the same cooperative unit. Although previous studies on lesion-containing duplexes suggest this to be a reasonable assumption (Vesnaver et al., 1989), measurements of the transition enthalpies via differential scanning calorimetry (DSC) are needed to test the veracity of this assumption for the duplexes studied here. Such measurements are in progress, with the preliminary data suggesting that this assumption is valid. In this connection, it should be noted that out parent Watson–Crick duplex contains a stretch of three deoxyguanosines. We previously have observed that calorimetric studies on duplexes with such regions yield unexpectedly low transition enthalpies (Breslauer et al., 1986). In fact, our preliminary DSC data on the GC duplex are consistent with this expectation. The traditional explanation for equilibria in which ΔH_{cal} is found to be lower than ΔH_{vH} is to suggest the existence of intermolecular association (e.g., aggregation). However, the NMR studies of Patel and co-workers, which were conducted at considerably higher concentrations, reveal no such behavior. This result is consistent with our observation that the ΔH_{vH} data, derived from the shape of the melting curves, are independent of concentration. Such concentration-independent behavior suggests that significant aggregation is unlikely. Interestingly, the van't Hoff transition enthalpies we derive from the shapes of the DSC thermograms are in excellent agreement with those derived from the shapes of the absorbance-monitored melting profiles, despite the unexpectedly reduced areas under the heat capacity curves (i.e., low ΔH_{cal} values). We are in the process of investigating the origins of these apparently conflicting observations. However, in the interim, we judge it to be appropriate to present and to interpret, with the qualifications noted, the van't Hoff enthalpy data we have measured for the four duplexes studied in this work.

The Lesion Affects the Differential Thermal Stability but Not the Differential Thermodynamic Stability of Duplexes with C and A Cross-Strand Partners. As noted earlier, the presence or absence of the modified guanine residue alters the influence of the cross-strand partner on duplex thermal stability. Specifically, placement of a C or an A residue

opposite an *unmodified* central guanine residue results in a significant difference in duplex thermal stability (ΔT_m = 6 °C for the GC versus the GA duplexes). By contrast, when the central guanine residue is modified to X, placement of a C or an A residue opposite X has little influence on the differential duplex thermal stabilities (ΔT_m = –0.9 °C for the XC versus XA duplexes). In other words, the presence of the lesion alters, and in this case reduces, the differential thermal stabilities of the duplexes with C and A cross-strand partners relative to the corresponding duplexes without the lesion. By contrast, as described below, the presence of the lesion does not alter the corresponding differential thermodynamic stabilities.

Using the van't Hoff transition enthalpies and the total strand concentration, values for ΔS_{vH} and ΔG_{vH} may be estimated (Marky & Breslauer, 1987). The resulting data are summarized in Table I. Because the van't Hoff treatment refers to an undefined mole unit and assumes a truly bimolecular process, these data are best interpreted by consideration of differences between duplexes rather than absolute numbers. This interpretation assumes implicitly that any deviation from two-state, bimolecular behavior is the same for each of the duplexes.

Recall that we find substantial differences in T_m and ΔH_{vH} for the parent Watson–Crick duplex, GC, and the mismatch duplex, GA (see Table I), with the GC duplex melting at a higher temperature and with a greater transition enthalpy. We now find that, due to compensation by favorable entropic effects, the net impact of the mismatch on the duplex thermodynamic stability, ΔG_{vH}, is minimized. To be specific, at 25 °C the differential stability ($\Delta\Delta G_{vH}$) between the parent GC duplex and the mismatch GA duplex is only 1.3 kcal/"mole", despite the significant differential thermal stability (ΔT_m = 6.2 °C) and differential transition enthalpy ($\Delta\Delta H_{vH}$ = 8.8 kcal/"mole"). This large enthalpy–entropy compensation, which minimizes the differential stability ($\Delta\Delta G_{vH}$) between the GC and GA duplexes, reflects the plasticity of DNA to accommodate structural perturbations in a manner that minimizes the net free energy cost. The difference in thermodynamic stability, $\Delta\Delta G_{vH}$, for the two corresponding duplexes with the modified guanine residue, XC and XA, also is 1.3 kca./"mole", a value identical to that which we observe for the differential stability between GC and GA. Thus, while there is a substantial destabilization of the duplex induced by the presence of the lesion [GC vs XC ($\Delta\Delta G_{vH}$ = 3.8 kcal/"mole") or GA vs XA ($\Delta\Delta G_{vH}$ = 3.8 kcal/"mole")], the relative or differential stability of duplexes with a C or an A residue opposite either a G or an X residue is unperturbed. This behavior contrasts with the influence of the lesion on the differential thermal stability of the duplex (ΔT_m), thereby emphasizing the necessity of going beyond the traditional T_m comparisons when assessing the thermodymamic impact of lesions.

Comparisons with Structural Data. Patel and co-workers have applied two-dimensional NMR techniques to elucidate distinct solution structures for a 9-mer duplex containing an XA base pair at acidic pH (Kouchakdjian et al., 1989) and basic pH (Kouchakdjian et al., 1990). Significantly, in these structural studies, the XA base pair resides in the same sequence context as in the duplex which we have studied. Consequently, as described below, we can make comparisons and propose correlations between Patel's structural results and our thermodynamic data.

CD Detection of the pH-Induced Structural Alterations of the XA Duplex. As noted earlier, NMR studies at acidic and basic pH have shown that the XA base pair, in the identical sequence context as studied here, exists in different conformations (Kouchakdjian et al., 1989, 1990). At acidic pH, the propano-dG of the XA base pair adopts a syn orientation, and the deoxyadenosine base is protonated. These pH-induced alterations provide the possibility at low pH of two hydrogen bonds between the X and A bases, while at basic pH, both the X and A bases are uncharged and in their anti orientations. As such, at basic pH, the X and A bases have the potential to form only one hydrogen bond, with the NMR data suggesting that the one possible H-bond does not form. Significantly, the optically-detected, pH-induced transition we observe in the CD spectra for the XA duplex (see above) parallels the NMR-detected, pH-induced structural transition. Furthermore, the pH-dependent increase we observe in the positive CD band near 280 nm for the XA duplex may reflect alterations in stacking of the exocyclic base with neighboring bases as suggested by Kouchakdjian et al. (1990) based on NMR data.

While casual examination of the apparent pK_a we observe for the pH-induced structural transition of the XA duplex (6.6) and that observed by Kouchakdjian et al. (1990) (7.6) might suggest a discrepancy, the values are actually not irreconcilable. To be specific, Kouchakdjian et al. (1990) appropriately correct for the isotope effect on the electrode response (Glasoe & Long, 1960). However, one also must correct for the isotope effect on the ionization constant of the adenine ring nitrogen (Giralt et al., 1983; Bundi & Wüthrich, 1979). When this is done, the reported apparent pK_a of 7.6 in D_2O actually corresponds to about 7 in H_2O. Furthermore, the CD observable is sensitive to the relative orientations of the base electronic transition dipoles, and as such is exquisitely sensitive to small perturbations in base stacking. Altered transition dipoles caused by protonation of a base also will be reflected in the CD spectra. By contrast, the NMR observable is dependent on the kinetics of exchange between the two structures. It is quite reasonable to assume that the relative weighting of the contributions of each structure to the average observable is different for these techniques and that a somewhat different apparent pK_a can be observed for the same process.

The Substantial pH-Induced Structural Alterations of the XA Duplex Are Thermodynamically Neutral. Under acidic conditions (pH 5.8), the NMR data reveal that all bases 5′ and 3′ to the lesion site are stacked into a right-handed helix. At the lesion site, the A residue is protonated and in the anti glycosidic conformation. By contrast, the X residue adopts a syn glycosidic conformation with the exocyclic, propane bridge protruding into the major groove. This conformation results in minimal disruption of the overall DNA helix. Taken together, the protonation of the A residue and the syn conformation of the modified base X permit formation of two potential hydrogen bonds between the bases in the low-pH form of the XA base pair.

Under basic conditions (pH 8.9), the lesion is incorporated into a right-handed helix with all bases stacked into the duplex. By contrast with the acid form, both the X and A residues exhibit the anti glycosidic conformation, and both residues are partially intercalated between bases on the partner strand. The exocyclic, propane bridge is directed toward the partner strand and stacked between the opposite A residue and its 3′ neighbor, while in the acid form it protrudes into the major groove. In the basic form, the immediately flanking base pairs are fully paired in the Watson–Crick motif but are separated by larger than usual distances due to the partial intercalation of the bases at the lesion site. With both X and A residues intercalated between stacked bases, base-pairing via hydrogen bonds is precluded at high pH, in contrast to the

protonated A, X syn, low-pH form where two hydrogen bonds are possible. Thus, at both acidic and basic pH, the bulky, exocyclic, propane bridge is accommodated into an overall right-handed and B-like DNA helix but with significantly different local structural perturbations at the lesion site, as just described. Interestingly, despite these substantial, local structural differences, we find, within experimental error, no dependence of the van't Hoff transition enthalpy on pH. If one makes the reasonable assumption that the high-temperature, final, melted, "random coil" states are energetically equivalent, then our data suggest that the high- and low-pH forms of the XA duplex are isoenthalpic, despite the local structural differences observed by NMR. In other words, the syn–anti interconversion, base protonation, and other associated structural changes do not result in a net change in the enthalpy of the duplex at low and high pH.

To assess the impact of these pH-induced structural alterations on the *thermodynamic* stability (ΔG_{vH}) of the XA duplex, we used our measurements of ΔH_{vH} and T_m to calculate the difference in free energy between the duplex with the X residue in the syn orientation (low-pH form) and the duplex with the X residue in the anti orientation (high-pH form). Due to differences in averaging the pH- and concentration-dependent data, this analysis yields numerical values slightly different from that listed in Table I. However, the relevant differential value remains unaltered. From the pH-dependent CD data, we estimate that at pH 6.0 the fraction of duplexes in the anti form is 0.20, while at pH 7.0 the corresponding fraction is 0.72. The T_m of XA at pH 6.0 is 52.9 °C, while at pH 7.0 it is 51.6 °C. From these data, we estimate that for the low-pH X(syn)A(anti) duplex $\Delta G_{25°C}$ = 13.8 kcal/"mole", while for the high-pH X(anti)A(anti) duplex $\Delta G_{25°C}$ = 13.4 kcal/"mole". Thus, the thermodynamic consequences of the syn–anti transformation, along with the associated structural alterations noted above, are minimal. This result suggests that DNA is capable of accommodating significant structural perturbations with minimal energetic costs.

Concluding Remarks. We have demonstrated that 1,N^2-propanodeoxyguanosine promotes alterations in duplex DNA which can be observed by circular dichroism. We showed that the lesion-induced structural alterations reduce the duplex thermal stability, the duplex transition enthalpy, and the duplex transition free energy. We also demonstrated that the presence of the modified guanine residue renders the duplex thermal stability insensitive to whether the cross-strand partner base is a C or an A residue, a result that contrasts with the behavior we observe with the two corresponding unmodified duplexes. In contradistinction, we find that the presence or absence of the modified guanine does *not* alter the influence of the cross-strand partner on the differential thermodynamic stabilities of the duplexes. In other words, the lesion alters the differential thermal stability (ΔT_m) but not the differential thermodynamic stability ($\Delta\Delta G_{vH}$) of duplexes with C and A cross-strand partners. This result emphasizes the necessity of going beyond traditional T_m measurements and comparisons when assessing the net thermodynamic impact of a lesion. We also have detected by CD an intriguing pH-dependent structural transition with an apparent pK_a near neutrality for the XA duplex which is absent in all the other duplexes. Because A residues are preferentially inserted opposite X adducts in vivo, this result suggests that the biological repair system may be confronted with a mixture of two structures under physiological conditions. This feature must be considered when developing models by which the repair enzymes recognize and selectively bind to such lesion-containing domains. Furthermore, we found the XA and XC duplexes to be thermodynamically similar. Consequently, the observed preference for insertion of A over C residues across from the lesion should not be rationalized in terms of thermodynamic differences between the final duplex states, and probably reflects properties of the DNA polymerase and the replication fork. Finally, we found the thermodynamic consequences of the substantial pH-induced, NMR-characterized structural alterations in the XA duplex (Kouchakdjian et al., 1989, 1990) to be minimal. This surprising result suggests that DNA may be sufficiently plastic so as to accommodate significant structural alterations in a compensating manner so as to result in a minimal net energetic cost.

REFERENCES

Aboul-ela, F., Koh, D., Tinoco, I., Jr., & Martin, F. H. (1985) *Nucleic Acids Res. 13*, 4811–4824.

Basu, A. K., & Essigmann, J. M. (1988) *Chem. Res. Toxicol. 1*, 1–18.

Breslauer, K. J., Sturtevant, J. M., & Tinoco, I., Jr. (1975) *J. Mol. Biol. 99*, 549–565.

Breslauer, K. J., Frank, R., Blöcker, H., & Marky, L. A. (1986) *Proc. Natl. Acad. Sci. U.S.A. 83*, 3746–3750.

Bundi, A., & Wüthrich, K. (1979) *Biopolymers 28*, 285–297.

Bush, C. A. (1974) in *Basic Principles in Nucleic Acid Chemistry* (T'so, P. O. P., Ed.) Vol. 2, pp 91–169, Academic, New York.

Cantor, C. R., & Schimmel, P. R. (1980) *Biophysical Chemistry*, W. H. Freeman & Co., San Francisco, CA.

Chung, F.-L., Young, R., & Hecht, S. S. (1984) *Cancer Res. 44*, 990–995.

Felsenfeld, G., & Rich, A. (1957) *Biochim. Biophys. Acta 26*, 457–468.

Gaffney, B. L., & Jones, R. A. (1989) *Biochemistry 28*, 5881–5889.

Giralt, E., Viladrich, R., & Pedroso, E. (1983) *Org. Magn. Reson. 21*, 208–213.

Glasoe, P. K., & Long, F. A. (1960) *J. Phys. Chem. 64*, 188–190.

Grollman, A. P. (1989) *Proc. Am. Assoc. Cancer Res. 30*, 682.

Huang, P., & Eisenberg, M. (1992) *Biochemistry 31*, 6518–6532.

Job, P. (1928) *Ann. Chim. (Paris) 9*, 113–134.

Kouchakdjian, M., Marinelli, E., Gao, X., Johnson, F., Grollman, A., & Patel, D. J. (1989) *Biochemistry 28*, 5647–5657.

Kouchakdjian, M., Eisenberg, M., Live, D., Marinelli, E., Grollman, A., & Patel, D. J. (1990) *Biochemistry 29*, 4456–4465.

Kouchakdjian, M., Eisenberg, M., Yarema, K., Basu, A., Essigmann, J., & Patel, D. J. (1991) *Biochemistry 30*, 1820–1828.

Marky, L. A., & Breslauer, K. J. (1987) *Biopolymers 26*, 1601–1620.

Marky, L. A., Kallenbach, N. R., McDonough, K. A., Seeman, N. C., & Breslauer, K. J. (1987) *Biopolymers 26*, 1621–1634.

Plum, G. E., Park, Y. W., Singleton, S., Dervan, P. B., & Breslauer, K. J. (1990) *Proc. Natl. Acad. Sci. U.S.A. 87*, 9436–9440.

Shapiro, R. (1969) *Ann. N.Y. Acad. Sci. 163*, 624–630.

Singer, B., & Grunberger, D. (1983) in *Molecular Biology of Mutagens and Carcinogens*, Plenum Press, New *York*.

Singer, B., & Bartsch, H. (1986) *The Role of Cyclic Nucleic Acid Adducts in Carcinogenesis and Mutagenesis*, No. 70, IARC Scientific Publications, Lyon, France.

Vesnaver, G., Chang, C.-N., Eisenberg, M., Grollman, A. P., & Breslauer, K. J. (1989) *Proc. Natl. Acad. Sci. U.S.A. 86*, 3614–3618.